Int. J. Heat Mass Transfer. Vol. 21, pp. 221–229. Pergamon Press 1978. Printed in Great Britain

THE CHARACTERISTICS OF HEAT EXCHANGERS USING HEAT PIPES OR THERMOSYPHONS

Y. LEE and A. BEDROSSIAN
Department of Mechanical Engineering, University of Ottawa, Ottawa, Canada

(*Received* 6 *December* 1976 *and in revised form* 12 *May* 1977)

Abstract—The characteristics of counter-flow heat exchanger units, using heat pipes or two-phase closed thermosyphons as the heat-transfer element, are studied experimentally and a simple analytical model was developed to predict the performance of such units using thermosyphons.

The maximum heat-transfer rate has a unique functional relationship between the ratio of two stream mass flow rates, and the ratio of heated to cooled lengths of the heat-transfer elements, regardless of element bundle geometries.

NOMENCLATURE

A, heat-transfer area;
B, constant, equation (10);
C_{sf}, constant, equation (12);
C_z, constant, equation (10);
c_p, specific heat at constant pressure;
d, diameter of heat-transfer elements;
g_c, conversion factor for units of force;
h, heat-transfer coefficient;
h_{fg}, latent heat of vaporization;
k, thermal conductivity;
L, length of the element;
L^+, length ratio, L_h/L_c;
m, mass flow;
Q_T, total heat-transfer rate of an exchanger;
q, heat-transfer rate of an element;
R, thermal resistance;
r, radius;
S_L, longitudinal-element pitch in a bank, Fig. 2;
S_T, transverse-element pitch in a bank, Fig. 2;
T, temperature;
U, overall heat-transfer coefficient of an exchanger;
u, fluid velocity through the minimum free area;
Y, dimensionless film thickness (r_δ/r_i);
Nu, Nusselt number, hd/k or Ud/k;
Pr, Prandtl number, $\mu c_p/k$;
Re, Reynolds number, ud/v;
Re^*, Reynolds number ratio, Re_h/Re_c;
β, dimensionless condensation parameter;
γ, specific weight;
θ, angle of orientation;
μ, dynamic viscosity;
v, kinematic viscosity;
σ, surface tension.

Superscripts

m, n, exponents, equation (10).

Subscripts

c, condenser side; cold;
g, geometric;
h, evaporator side; hot;
i, inner side of the element;
m, logarithmic mean;
o, outerside of the element;
p, individual element;
s, saturation;
T, total;
w, wall;
ci, inlet cold-side fluid stream;
hi, inlet hot-side fluid stream;
vap, vapor;
δ, at the film boundary.

INTRODUCTION

INCREASING fuel cost and energy conservation are two of the most important considerations to be taken in new heat exchanger design, and modern compact heat exchangers with as much as 4900 m^2 of surface per m^3 of exchanger, very often accommodate these important requirements. For low temperature differences, such as in the case of recovering heat from exhaust gas streams, however, these units become impractical. In some other cases, design conditions may dictate that two fluids must be physically separated to avoid any cross contamination between two fluids in a heat exchanger. Heat exchangers, having two-phase closed thermosyphons or heat pipes as heat-transfer elements within, may actually be good examples to accommodate these particular design constraints.

Although the heat pipes and two-phase closed thermosyphons are similar, there is an important difference in the mechanism of condensate return in these elements. A heat pipe relies on the capillary action of the internal wick and the working fluid, whereas a thermosyphon employs an external force field, such as gravity, centrifugal force, etc. for the condensate return to the evaporator.

The hydrodynamic and thermal aspects of individual elements have been extensively studied for heat pipes and to a lesser degree for two-phase closed thermosyphons, but it appears that the study to predict the overall performance of heat exchangers, having a bank of such heat-transfer elements within, is confined to very few [1, 2]. These studies are preliminary in nature and are all concerned with those having heat pipes only. Some performance data and possible application of such heat exchangers are included in a monograph recently published [3]. An extensive review on the thermosyphon technology is also made available by Japikse [4].

In the present paper, a study has been made on the characteristics of such heat exchangers experimentally and a simple analytical model was developed to predict the optimum design condition for units using two-phase closed thermosyphons. Although the study is applicable to both parallel and counter flow heat exchangers, only the latter is investigated in the present paper.

ANALYSIS

Three approaches are available to predict heat-transfer performance of heat exchangers using two-phase closed thermosyphons or heat pipes. The first method, based on a conductance model, is to estimate heat-transfer coefficients involved in each process, and is adopted in the present study.

The second method is suitable mainly for the prediction of the maximum heat-transfer rate of a given thermosyphon element. This is done by estimating the rate of mass transport based on a force balance within the element [5] but it is not really adoptable for the analysis of the overall heat-transfer performance of heat exchangers under a given operating condition.

The third is the method developed by Kays and London [6], using the effectiveness-number of transfer units, applied especially in liquid-coupled indirect type heat exchangers. Here, the thermosyphons or heat pipes in the heat exchanger core, can be considered as the pumped fluid loop which couples the hot side and cold side. However, this method is not easily adaptable to the case studied here.

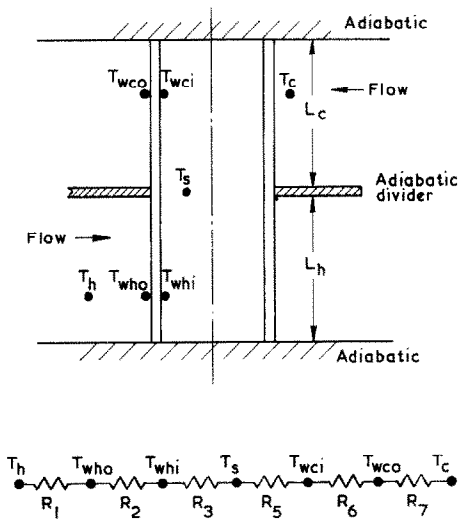

FIG. 1. An ideal model.

Although the first method may imply that only rate equations are required in the analysis, the principle of energy-balance must be included as well. The method of the analysis used can be applicable for both cases having heat pipes and two-phase closed thermosyphons, but only the latter is considered in the present study.

Assuming that the axial conduction through the tube wall is negligible, the following equations for the ideal model shown in Fig. 1 can be written for steady state operations:

$$q_p = \left| \frac{1}{R} (T_h - T_c) \right|_{\text{if}} \tag{1}$$

where

$$R = \sum_{j=1}^{7} R_j = R_4 \tag{2}$$

$$R_1 = \frac{1}{h_1 A_{ho}} \tag{3}$$

$$R_2 = \frac{1}{2\pi k L_h} \ln\left(\frac{r_o}{r_i}\right) \tag{4}$$

$$R_3 = \frac{1}{h_3 A_{hi}} \tag{5}$$

$$R_5 = \frac{1}{h_5 A_{ci}} \tag{6}$$

$$R_6 = \frac{1}{2\pi k L_c} \ln\left(\frac{r_o}{r_i}\right) \tag{7}$$

$$R_7 = \frac{1}{h_7 A_{co}} \tag{8}$$

and the total heat-transfer rate of the entire heat exchanger is defined by:

$$Q_T = \sum_{p=1}^{n} q_p = A_f U \Delta T_m. \tag{9}$$

The outer h_1 and h_7 in R_1 and R_7, respectively, are not strongly affected by the temperature and are estimated from the standard correlation for the fluid flow normal to the bank or rod bundles given by:

$$Nu = B \cdot C_Z Re^m Pr^n \tag{10}$$

where B and m are functions of longitudinal and transverse pitch ratios; C_Z a correction factors for the geometry and the number of rows in the bank of heat-transfer elements; and n is about 1/3 [7].

The thermal resistances R_2 and R_6 can be rather accurately calculated with standard conduction heat transfer.

The resistance R_4 only appears when the flow inside the thermosyphon reaches its choking condition, and then it becomes the controlling factor.

The values of the internal evaporator and condenser heat-transfer coefficients, h_3 and h_5, respectively, are

the most difficult to estimate. For h_5, the analytical expression given in [5], cannot be used as it is only for the maximum heat-transfer rate from a given thermosyphon. Therefore, for the condenser section in the present study, the Martinelli's expression given below was used [8]:

$$\frac{h_5 d_i}{k} = \frac{1}{\beta}\left[\tfrac{1}{4} - Y^2 + \tfrac{3}{4}Y^4 - Y^4 \ln Y\right] \qquad (11)$$

where

$$Y = r_\delta / r_i$$

$$\beta = Y^4 \ln Y\left(\frac{\ln Y}{2} - \tfrac{1}{2}\right) + \frac{Y^4}{8} + Y^2\left(\frac{\ln Y}{2} - \tfrac{1}{4}\right) + \tfrac{1}{8} = \frac{2kv(T_s - T_w)}{g_c(\gamma - \gamma_{vap})h_{fg} r_i^4}.$$

For h_3, the evaporating section of the thermosyphon, the Rohsenow's correlation for natural convection boiling [9] given by:

$$\frac{c_p(T_w - T_s)}{h_{fg}} = C_{sf} Pr^{1.7}\left[\frac{h(T_w - T_s)}{\mu h_{fg}}\left(\frac{\sigma}{\gamma - \gamma_{vap}}\right)^{1/2}\right]^{0.33} \qquad (12)$$

was used. Here, all properties are evaluated at the saturation temperature, T_s and the constant C_{st} from [10].

Equations (11) and (12) indicate that not only a knowledge of the temperature drop is necessary, but also a fairly accurate value of the saturation temperation, T_s, must be known.

Therefore, to satisfy all these concomitant requirements, iterative methods had to be used to predict the overall performance of the heat exchanger.

EXPERIMENTS

A schematic diagram of the experimental setup is shown in Fig. 2. The test section consists of two rectangular air ducts, traversed at the middle portion by a bank of heat-transfer elements (i.e. thermosyphons or heat pipes). Figure 2 also shows the locations of thermocouples, with respect to the segmented baffles which mix the air stream to achieve a uniform temperature distribution. The system can be used for both counterflow and parallel-flow arrangements, and the possible leakage between the two streams is prevented by an air-tight partition.

The flow rates are measured by two calibrated orifice plates located downstream from the test section on 102-mm dia circular portions of the air ducts. Provisions are also made to measure the pressure drops across the test section.

Air temperature measurements are made by calibrated, radiation shielded beads of copper–constantan junction. At every temperature measuring station, each duct cross-section is traversed along two perpendicular directions, and the average of at least five thermocouples are provided at each measuring station to obtain a meaningful bulk temperature at that particular cross-section.

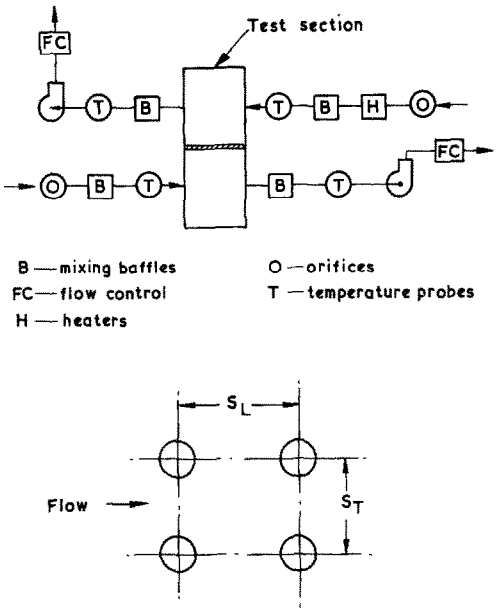

FIG. 2. Schematic diagram of the test apparatus and element bundle arrangement.

An additional special feature of the test section is that the entire section can be pivoted about a fixed reference axis, to change the orientation of the heat-transfer element bank in respect to the gravitational field. The angle $\theta = 90°$ indicates that the elements are parallel to the direction of the gravitation, and that the evaporator section is below the condenser section.

Table 1. Characteristics of heat-transfer elements

Element	Length (mm)	Outside diameter (mm)	Wall thickness (mm)	Symbols
Thermo-syphons	305	12.7	0.84	TS
Heat pipes	305	12.7	0.82	HP†

†Model No. CWS 5012, see footnote.

Although the analysis is confined to a heat exchanger using thermosyphons, a set of purchased heat pipes* were used for comparison. The two-phase closed thermosyphons used in the study were developed and manufactured by the authors' institute. The main characteristics of these two heat-transfer elements are summarised in Table 1.

All heat pipes and thermosyphons are made of hard-drawn copper tubing and the working fluid for both is distilled water. The amount of working fluid in the thermosyphons is about 15% of the total inner volume of the elements according to the findings of [5], which made an experimental study on the effect of the quantity of working fluid filling on the heat-transfer performance of the element.

*Isothermics Inc., P.O. Box 86, Augusto, NJ 07822, U.S.A.

To test the effect of element bank geometry on the overall performance, the following different element spacings are used:

In-line elements:
- 5×4 rows
- total No. of elements ... 20
- total heat-transfer area, $L^+ = 1 \ldots 0.122\ m^2$

Staggered elements:
- 4–5–4–5 (4 rows)
- total No. of elements ... 18
- total heat-transfer area, $L^+ = 1 \ldots 0.109\ m^2$

$S_L = 38.1$ mm; $S_T = 16$, 25.4 and 38.1 mm.

The ratio, L^+, of heated-length, (L_h), to cooled-length (L_c), is one of important parameters and provisions are made in the design of the test apparatus to accomodate this particular requirement.

RESULTS AND DISCUSSION

Correlation of the test results were attempted, using various kinds of the characteristic length to be used in the non-dimensional parameters, but it seems that the diameter of the heat-transfer element is the best choice.

The predicted overall heat-transfer coefficients, U, for a given condition are compared with the experimental results in Fig. 3. The curve AA is obtained using equation (10) with Grimison's values [11] of B and m which are needed for equations (3) and (8). As can be seen from the figure, the agreement between the analysis and experiment is very poor except for the region near $Re_c \doteq 3000$.

It was thought that the poor agreement could have resulted from two sources in the analysis. One is the values of B and m in equation (10) which determines the values of R_1 and R_7, and the other, the constant, C_{sf}, in the Rohsenow's correlation given by equation (12). Therefore firstly, the computation was repeated with different values for the constant, C_{sf}, keeping the others the same. However, it showed that the effect of changes in the value of C_{sf} on the final overall coefficient, was very insensitive.

Secondly, the computation was repeated with the different values of B and m in equation (10), keeping the rest the same, and with the values of B and m of 0.009 and 1.05, respectively. The prediction follows the experimental trend very closely, as shown by the curve CC in Fig. 3.

Recent studies [12, 13] showed that the Grimison's correlation does not reflect several important parameters affecting the heat-transfer process. The study of these variations is beyond the scope of the present work, but throughout the analysis, the corrected values of B and m, given as 0.009 and 1.050, respectively, were used in equation (10) and as it can be seen from Figs. 3, 9 and 10, the agreement between the prediction and experimental results is very good.

At this point, it must be pointed out that, unlike a simple convection heat-transfer process, the heat-transfer process in the heat exchanger, using the two-phase closed thermosyphons or heat pipes, is quite sensitive to the temperature range and to the overall temperature difference of the total system due to the fact that the process involves two-phase phenomena. This is clearly demonstrated in Fig. 4, where the effects of the initial temperature of the one fluid stream and the temperature difference, $T_{hc} - T_{ci}$, on the overall heat-transfer coefficients, U, at different conditions are illustrated. Therefore, throughout the experiment, T_{ci} was kept at 21 ± 1°C, and ΔT at 65 ± 10°C, so that the uncertainties introduced by the dependancy on temperature can be kept within the acceptable tolerance. The predictions which were compared with the experimental results, were naturally kept at the same T_{ci} and ΔT used in the experiment.

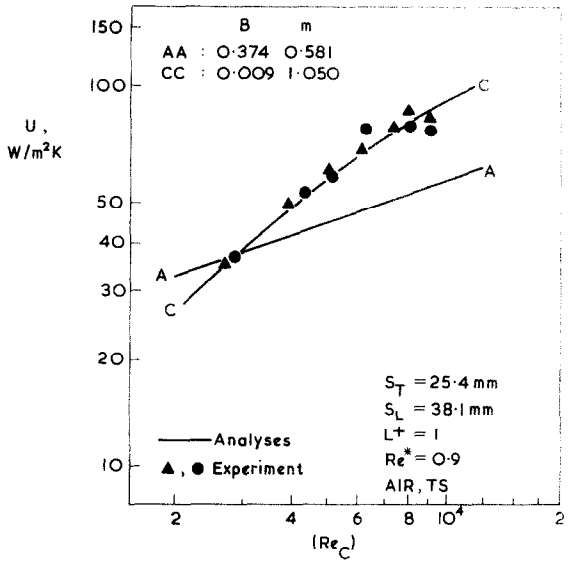

FIG. 3. Comparison of analysis with experimental results, in-line bundle geometry.

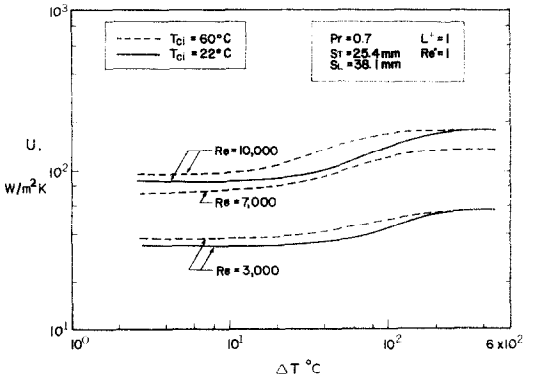

FIG. 4. Effect of temperature, in-line bundle geometry.

Effects of Reynolds number and of the ratios Re* *and* L^+

In a heat exchanger, the heat-transfer rate from one stream to the other not only depends on the Reynolds numbers of the two streams, but also on the ratio of the two Reynolds numbers of the streams, $Re^* = Re_h/Re_c$. The heat exchanger studied here is no exception and their effects are shown in Fig. 5.

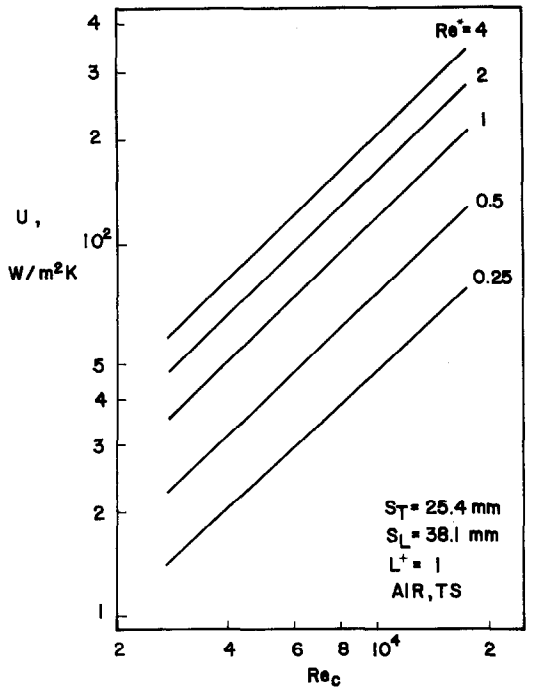

FIG. 5. Effects of Reynolds number and Re^*, in-line bundle geometry.

The trend shown in the figure, however, can be quite misleading. For the range of moderate Reynolds numbers, as in the case of Fig. 5, it is true that increasing the Reynolds number for a given value of Re^* results in a higher value of U. But, if we were to increase the Reynolds number to a much higher order of magnitude for a given Prandtl number, one can see that the effect of the Reynolds number on U becomes asymptotic, as shown in Fig. 6 (the effect of Pr in conjunction with Re_c will be discussed later). The explanation is simple; the heat-transfer process from the hot stream to the cold stream in the present heat exchanger is governed by equation (1), and the individual thermal resistance plays its own role depending on its magnitude. Figure 6 indicates that there is a maximum heat-transfer rate for a particular design of the heat-transfer elements at a given condition. This implies that the addition of a number of fins to the outside surface of heat-transfer elements would improve the overall heat-transfer process, especially at low Reynolds numbers, but there is a limit beyond which an increase in the number of fins would not necessarily result in a higher value of U, especially at high Reynolds numbers.

Coupled to this effect is that of Re^*. For a given value of Re_c, the higher the value of Re^*, the larger the value of U. It seems to imply that increasing the evaporator side heat-transfer increases the overall performance of the heat exchanger and vice versa. However, the effect of Re^* on the overall heat-transfer coefficients is much more complicated due to the fact that the ratio of heated-length to cooled-length, $L^+ = L_h/L_c$, of the heat-transfer elements also affects the heat-transfer process.

If we were to change the value of L^+, we can no longer consider the overall heat-transfer rate per unit area, because the heat-transfer area is not unique anymore.

As discussed previously, the total thermal resistance is the summation of six different resistance governed by the conditions of R_4 and each of which, is specified by its particular heat-transfer mechanism. For $L^+ = 1$, where the outer surface area of the condenser equals the evaporator outside surface area (the diameters being the same), U_c becomes U_h. For values of L^+ other than 1, neither U_c nor U_h, which are based on the condenser and the evaporator outside areas, respectively, would give any representative picture of the change in the performance of the system, associated with the relative change of areas as can be seen in Fig. 7. Since both evaporator and condenser side areas must strongly affect the performance of the system, both areas should be included in the definition of the overall heat-transfer coefficient. Since the question may be treated as a matter of definition, one may use either arithmetic, geometric or logarithmic means of the two areas in the definition of U, but none of these reflects real changes in the performance of the system, as shown in Fig. 7. Therefore, although the concept of overall heat-transfer coefficient is preferred (and for

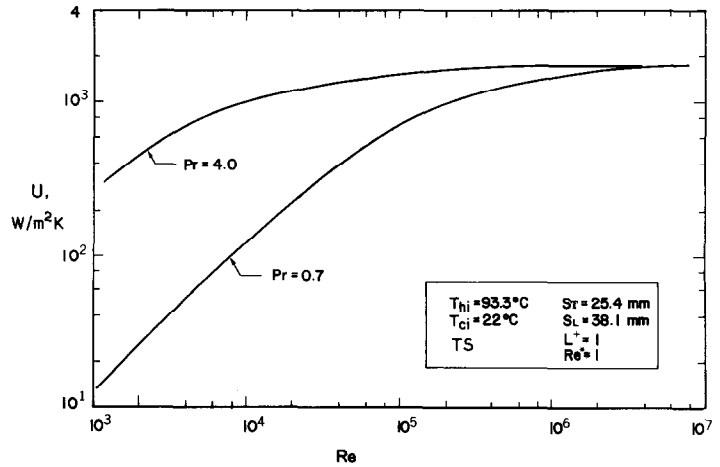

FIG. 6. Effects of Reynolds and Prandtl number, in-line bundle geometry.

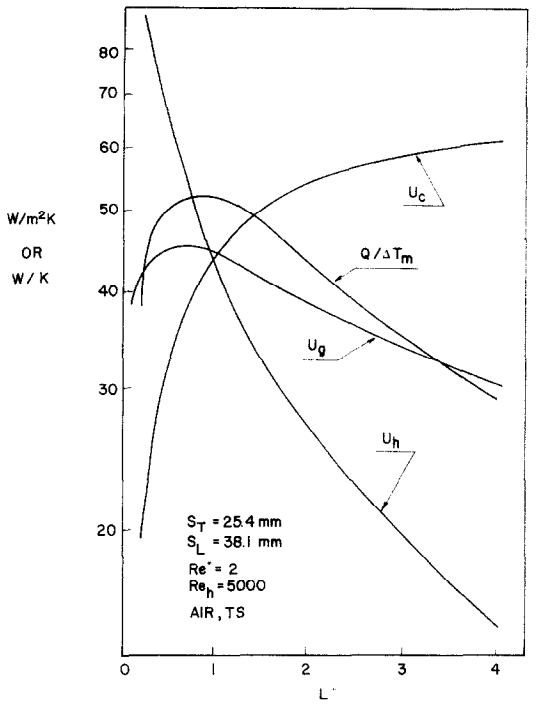

FIG. 7. Definition of heat conductance.

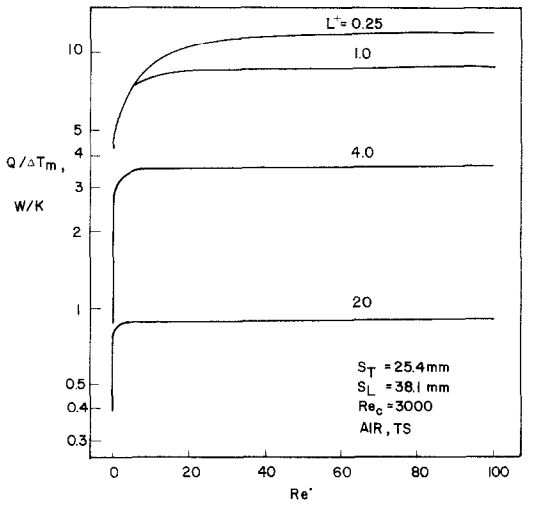

FIG. 8. Effects of L^+ and Re^*, in-line bundle geometry.

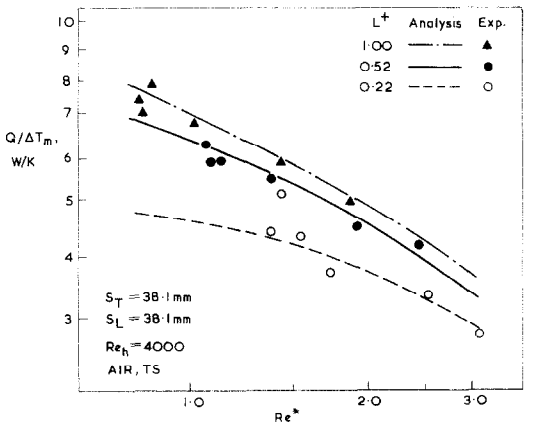

FIG. 9. Effects of L^+ and Re^*, comparison of analysis with experimental results, in-line bundle geometry.

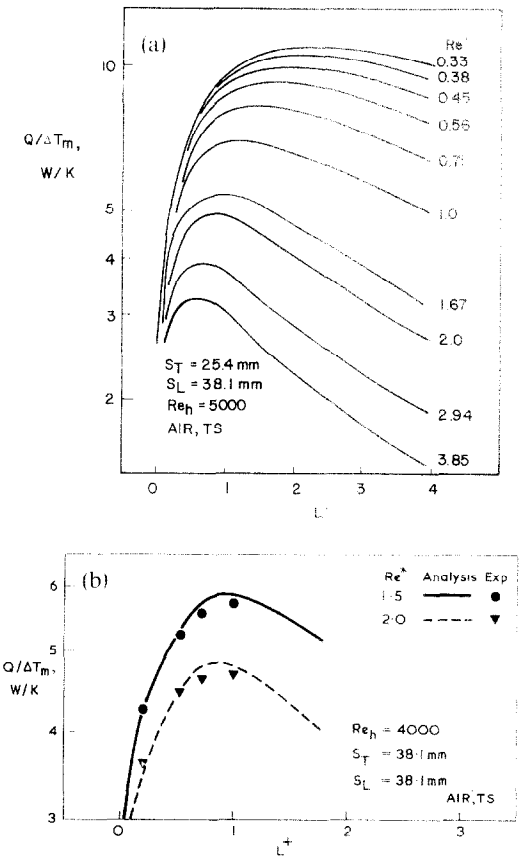

FIG. 10. (a) Relationship between Re^* and L^+, in-line bundle geometry. (b) Relationship between Re^* and L^+, comparison of experimental results with analysis, in-line bundle geometry.

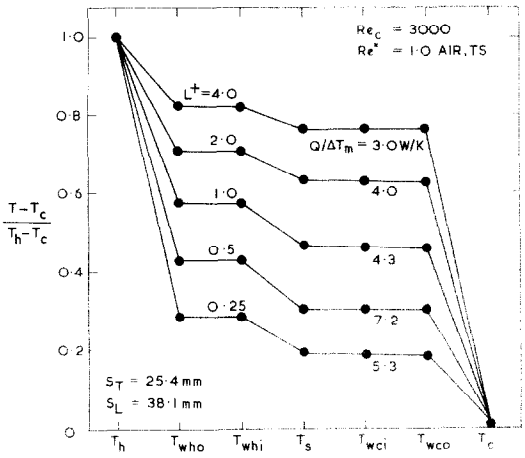

FIG. 11. Temperature distribution of an ideal element, in-line bundle geometry.

$L^+ = 1$, the results are always presented in U), for the values of L^+ other than 1, the overall conductance $Q/\Delta T_m$ seems to be the proper choice, as are used in Figs. 8–12.

Figure 8, where the value of Re_c was fixed, shows that once the value of L^+ is specified, there seems to be a point beyond which the overall heat-transfer rate does not improve with increasing Re^*. This trend is

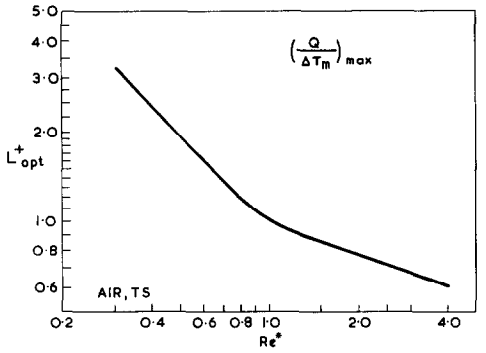

FIG. 12. The optimum relation between L^+ and Re^*.

similar to those shown in Fig. 6. The comparison with the experimental results are shown in Fig. 9, where the value of Re_h, not Re_c, was fixed at 4000. Considering the complexity involved in the experiment and the assumptions made in the analysis, the agreement is good. Now, if we were to fix the value of Re^* (i.e. the relative mass flows of the two streams are fixed) and change the value of L^+, we obtain the trend shown in Figs. 10(a) and (b). It can be seen that an increase in the hot-side area does not necessarily lead to higher performance. This can be better illustrated by plotting the temperature drops across the single heat-transfer element, as shown in Fig. 11. It is seen that for $Re^* = 1$, the optimum L^+ is also unity as is obvious from the fact that $R_1 = R_7$. If $R_1 \neq R_7$, as a result of $Re^* \neq 1$ and/or $L^+ \neq 1$, there must exist a unique relation between Re^* and L^+, which will give the maximum conductance for a given geometry of heat exchanger. The results of appropriate calculation are shown in Fig. 12. It is seen from the computation that the optimum relation shown in Fig. 12 holds for different flow rates and is independent of the heat-transfer element bank geometry.

Effect of stream Prandtl number

As was shown in Fig. 6, the relative magnitude of six thermal resistances involved in a thermosyphon decide the overall heat-transfer performance of the system. Increase in fluid stream Prandtl number implies, in general, a reduction in R_1 and R_7, and their effects are shown in Fig. 13. However, it must be stressed that to extrapolate the trend shown in Fig. 13 to a higher Reynolds number, together with the different temperature range, would be misleading as the relative role of the individual thermal resistance dictates the overall performance, as shown in Fig. 6. The Prandtl number shown in Fig. 13 was evaluated at the arithmetic average temperature of hot and cold streams.

Effects of bank geometry

The overall heat-transfer coefficients for staggered systems, are slightly higher than those for an in-line bank of thermosyphons. The trend was expected because the surface heat-transfer coefficient of the former is greater than that of latter at a given mass flow rate through the minimum free area. But again, these are governed by the relationships already discussed.

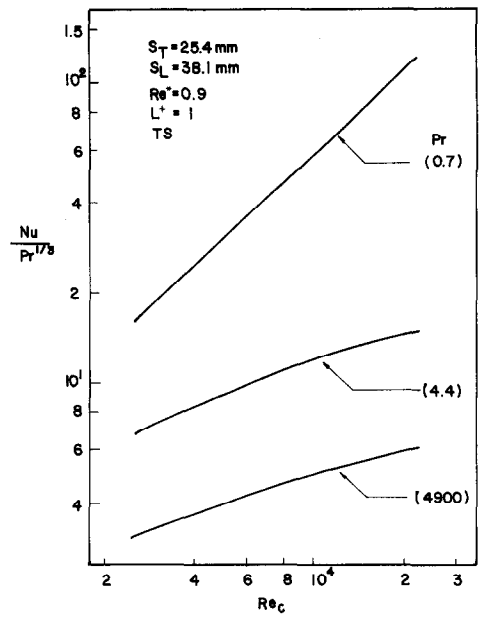

FIG. 13. Effect of Prandtl number, in-line bundle geometry.

The effect of the transverse spacing on the overall heat-transfer coefficient of the present system is quite different. As mentioned above, the Reynolds number is defined with the diameter of the element as the physical characteristic length, and the flow rate through the minimum free area as the mass flow rate. The marked increase in the Reynolds number due to the small free area for a given mass flow rate, did not result in higher values of the overall heat-transfer coefficient. As discussed previously, the heat-transfer processes involved are such that h_1 and h_7 have only a limited role over the performance of the two-phase heat-transfer elements. The trends are similar to those so far discussed for all the geometries studied, and the agreement between the prediction and the experiment is comparable to those shown in Figs. 3, 9 and 10(b).

Effects of element orientation

The effects of the heat-transfer element orientation of the system to the force field are shown in Fig. 14. Whereas the effect on the performance of the system

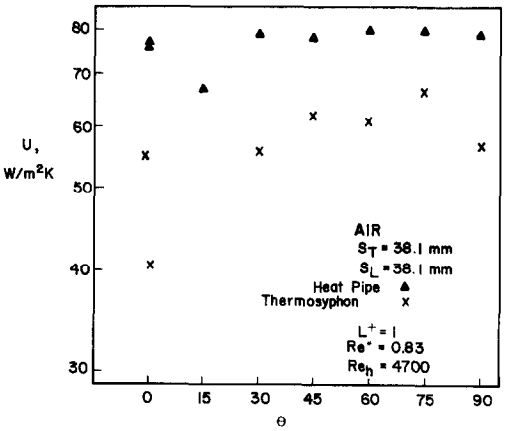

FIG. 14. Effect of orientation, in-line bundle geometry.

with heat pipes are negligible, it is quite significant for that with thermosyphons, especially near the horizontal position. It shows that the capillary action was dominant for the former.

From the experimental results, some of which are illustrated in Fig. 14, it was observed that the overall heat-transfer coefficients of the system with heat pipes were about 40% higher than those of the system with thermosyphons. However, the heat pipe used in the study is only one of many designs, and the comparison should not be taken to be universal.

The differences of response to orientation may allow designers to choose for particular applications. For instance, the characteristics of thermosyphons can be comparable to an electric diode, and this cut-off feature can be used in permafrost preservation [14].

Additional comments

In general, heat exchanger data may be presented by heat exchanger effectiveness [6] which depends upon the exchanger flow configuration, the capacity rate (mc_p) ratio of the two stream fluids and the NTU (number of transfer unit). Only for simple cases, the functional relation of NTU can be determined by solving appropriate differential equations.

A quantitative comparison of the present system with those of conventional systems was not performed, since the NTU of the present test exchanger is always smaller than 0.5 due to limited available heat-transfer area. In practice, the preferred values of NTU fall between 3 and 4, since in this range, close to 90% effectiveness is attained.

Therefore, it is obvious from the present study that one has to increase the NTU of the system, by an increase in available heat-transfer surface areas by such as adding the number of fins to the heat transfer elements. However, there must be an optical condition and this can be predicted by the method of the analysis used in the present study.

CONCLUSIONS

The following conclusions can be drawn from the present study:

1. A simple iterative calculation can predict the performance of heat exchangers having two-phase closed thermosyphons fairly well, with the correlation for the surface heat-transfer coefficients properly corrected, using available empirical information.

2. The maximum heat transfer of the unit has a unique functional relationship between L^+ and R^*, as shown in Fig. 12, regardless of element bank geometries.

3. The bank arrangement of the two-phase heat-transfer elements has comparable effects on the overall heat-transfer coefficients of the unit, as on the surface heat-transfer coefficients of simple convective cross-flow systems.

4. The effect of increasing Prandtl number and/or Reynolds number of any of two fluid streams, is to increase the overall heat-transfer coefficient up to a certain limit.

5. The optimum number of fins to be added to the surface of heat-transfer elements can be determined by the method used in the present analysis.

6. The effect of element orientation to the gravitational field is much more pronounced for thermosyphons than for heat pipes.

Acknowledgement—This work was supported by Imperial Oil Enterprises Limited, of Sarnia, Ontario, Canada.

REFERENCES

1. C. C. Silverstein, Heat pipe gas turbine regenerators, ASME paper 68-WA/GT-7, ASME Winter Annual Meeting, New York, 1–5 December (1968).
2. K. T. Feldman and D. C. Lu, Preliminary design study of heat pipe heat exchangers, in *Proceedings of the 2nd International Heat Pipe Conference, Bologna, Italy*, pp. 451–461 (1976).
3. P. D. Dunn and D. A. Reay, *Heat Pipes*. Pergamon Press, Oxford (1976).
4. D. Japiske, Advances in thermosyphon technology, in *Advances in Heat Transfer*, Vol. 3, pp. 2–111. Academic Press, New York (1973).
5. Y. Lee and U. Mital, A two-phase closed thermosyphon, *Int. J. Heat Mass Transfer* **15**, 1965–1707 (1972).
6. W. M. Kays and A. L. London, *Compact Heat Exchangers*. McGraw-Hill, New York (1964).
7. E. R. G. Eckert and R. M. Drake, Jr, *Analysis of Heat and Mass Transfer*, p. 414. McGraw-Hill, New York (1972).
8. L. M. K. Boelter, V. H. Cherry, H. A. Johnson and R. C. Martinelli, *Heat Transfer Notes*, pp. 559–562. McGraw-Hill, New York (1965).
9. W. M. Rohsenow, A method of correlating heat transfer data for surface boiling liquids, *Trans. Am. Soc. Mech. Engrs* **74**, 963–976 (1952).
10. L. S. Tong, *Boiling Heat Transfer and Two Phase Flow*. John Wiley, New York (1965).
11. E. D. Grimison, Correlation and utilization of new data on flow resistance and heat transfer of gases over tube banks, *Trans. Am. Soc. Mech. Engrs* **53**, 583–594 (1947).
12. B. Gebhart, *Heat Transfer*, p. 276, 2nd edn. McGraw-Hill, New York (1971).
13. Y. Lee and S. G. Kakade, Effect of peripheral wall conduction on heat transfer from a cylinder in cross flow, *Int. J. Heat Mass Transfer* **19**, 1031–1047 (1976).
14. Cryo-anchor statilizers, Bulletin, McDonnel-Douglas Astronautics Co., Washington (1975).

CARACTERISTIQUES DES ECHANGEURS THERMIQUES UTILISANT DES CALODUCS OU DES THERMOSIPHONS

Résumé—On étudie expérimentalement les caractéristiques des échangeurs thermiques à contrecourant utilisant des caloducs ou des thermosiphons fermés à deux phases comme élément de transfert de chaleur. Un modèle analytique simple est développé pour évaluer les performances de telles unités à thermosiphons. Le flux thermique maximal, fonction du rapport des flux massiques des deux écoulements et du rapport des longueurs chaudes et froides des éléments, est indifférent aux géométries des grappes d'éléments.

DIE EIGENSCHAFTEN VON WÄRMEAUSTAUSCHERN AUS WÄRMEROHREN ODER THERMOSIPHONS

Zusammenfassung—Die Eigenschaften von Gegenstrom-Wärmeaustauschern, welche Wärmerohre oder geschlossene Zwei-Phasen-Thermosiphons als Wärmeübertragungselemente benutzen, werden experimentell untersucht. Außerdem wurde ein einfaches analytisches Modell entwickelt, um die Leistung von solchen Apparaten mit Thermosiphons vorherzusagen. Die maximale Wärmeübertragungsleistung hat einen einzigen funktionalen Zusammenhang mit den beiden Massenströmen und dem Verhältnis von erhitzter zu gekühlter Länge des Wärmeübertragungselements, unabhängig von der Bündelgeometrie des Elementes.

ХАРАКТЕРИСТИКИ ТЕПЛООБМЕННИКОВ, ОСНОВАННЫХ НА ИСПОЛЬЗОВАНИИ ТЕПЛОВЫХ ТРУБ ИЛИ ТЕРМОСИФОНОВ

Аннотация — Проведено экспериментальное исследование противоточных теплообменников основанных на использовании тепловых труб или двухфазных замкнутых термосифонов в качестве теплообменного элемента; разработана простая аналитическая модель расчета рабочего режима таких установок с термосифонами.

Максимальная скорость теплообмена представляет собой функциональную зависимость между отношением двух массовых расходов и отношением длин нагретого и охлажденного участков в теплообменных элементах без учета их геометрии.